

Polygenic Risk for Schizophrenia Influences Cortical Gyrification in 2 Independent General Populations

Bing Liu^{1,2}, Xiaolong Zhang^{1,2}, Yue Cui^{1,2}, Wen Qin⁴, Yan Tao^{1,2}, Jin Li^{1,2}, Chunshui Yu⁴, and Tianzi Jiang^{*,1,2,3,5,6}

¹Brainnetome Center, Institute of Automation, Chinese Academy of Sciences, Beijing, China; ²National Laboratory of Pattern Recognition, Institute of Automation, Chinese Academy of Sciences, Beijing, China; ³Center for Excellence in Brain Science and Intelligence Technology, Institute of Automation, Chinese Academy of Sciences, Beijing, China; ⁴Department of Radiology, Tianjin Medical University General Hospital, Tianjin, China; ⁵Queensland Brain Institute, The University of Queensland, Brisbane, Australia; ⁶Key Laboratory for NeuroInformation of Ministry of Education, School of Life Science and Technology, University of Electronic Science and Technology of China, Chengdu, China

*To whom correspondence should be addressed; Brainnetome Center, Institute of Automation, Chinese Academy of Sciences, Zhongguancun East Road 95, Haidian District, Beijing 100190, China; tel: +86-10-8254-4778, fax: +86-10-8254-4777, e-mail: tjiangtz@nlpr.ia.ac.cn

Schizophrenia is highly heritable, whereas the effect of each genetic variant is very weak. Since clinical heterogeneity and complexity of schizophrenia is high, considerable effort has been made to relate genetic variants to underlying neurobiological aspects of schizophrenia (endophenotypes). Given the polygenic nature of schizophrenia, our goal was to form a measure of additive genetic risk and explore its relationship to cortical morphology. Utilizing the data from a recent genome-wide association study that included nearly 37 000 cases of schizophrenia, we computed a polygenic risk score (PGRS) for each subject in 2 independent and healthy general populations. We then investigated the effect of polygenic risk for schizophrenia on cortical gyrification calculated from 3.0T structural imaging data in the discovery dataset ($N = 315$) and replication dataset ($N = 357$). We found a consistent effect of the polygenic risk for schizophrenia on cortical gyrification in the inferior parietal lobules in 2 independent general-population samples. A higher PGRS was significantly associated with a lower local gyrification index in the bilateral inferior parietal lobules, where case-control differences have been reported in previous studies on schizophrenia. Our findings strongly support the effectiveness of both PGRSs and endophenotypes in establishing the genetic architecture of psychiatry. Our findings may provide some implications regarding individual differences in the genetic risk for schizophrenia to cortical morphology and brain development.

Key words: schizophrenia/polygenic risk score/cortical gyrification/inferior parietal lobule

Introduction

Although schizophrenia has been proven to be highly heritable,¹ the effects of specific variants are very small,² and it is difficult to obtain consistent results.³ This is partly because of its clinical heterogeneity and the complexity of its phenotypes along with their high degree of polygenic modulation.¹ Efforts have been made to compute polygenic risk score (PGRS) which could better capture the polygenic nature of complex disorders. A PGRS is based on the additive effects of a large number of disease-related genetic variants that individually have weak effects⁴ and allows the statistical power of large genome-wide association studies (GWAS) to be applied to small samples.^{5,6} The PGRS can then be used to investigate the effects of the cumulative genetic risk for the disorder on various phenotypes.⁷

The schizophrenia PGRS has been reported to be correlated with quantitative symptoms scales,⁸ cognitive performance,^{9,10} and neuroimaging measures.^{11–15} For example, increased schizophrenia polygenic risk predicts neurocognitive fluctuations in the general population.⁹ Specifically the polygenic risk for schizophrenia was associated with working memory-related prefrontal brain activation, a well-established intermediate phenotype for schizophrenia, in both schizophrenics and normal controls.¹² Efforts are also made to investigate the association between PGRS and brain volume.^{13–15} But until now, to the best of our knowledge, no study has investigated the effect of polygenic risk for schizophrenia on cortical morphology, the abnormality of which is associated with schizophrenia.^{16,17}

To establish the underlying genetic architecture of psychiatric disorders and identify the neural mechanisms that link genotypes to a clinical syndrome, endophenotype strategies have been increasingly employed.¹⁸ Endophenotypes, which are thought to be more closely related to the neurobiological activity of genes than clinical diagnosis, may provide footholds for studying the genetic underpinnings of a disorder.¹⁹ Gyrification refers to the pattern and degree of cortical folding and has been chosen as an candidate endophenotype for schizophrenia.²⁰ Gyrification can be measured by local gyrification index (LGI), which is a metric that quantifies cortical folding in a 3-dimensional approach by calculating the amount of cortex buried within the sulcal folds as compared with the amount of cortex visible on the outer surface of the brain.^{21,22} A higher value of LGI represents extensive folding whereas a lower value reflects a relatively flat cortex. The LGI was specifically designed to identify early defects in cortical development, was employed in our research.

In this study, we examined the correlation between the cumulative genetic risk for schizophrenia and cortical gyrification in 2 independent, general-population samples. The PGRS was derived from the largest (to our knowledge) GWAS of schizophrenia by the Schizophrenia Working Group of the Psychiatric Genomics Consortium.²³ We hypothesized that increased genetic risk for schizophrenia would be associated with disrupted cortical gyrification in areas, such as inferior parietal lobules (IPL),¹⁷ precentral gyrus,²⁴ and prefrontal cortex,²⁵ where case-control differences have been reported in previous studies on schizophrenia.

Methods

Participants

Discovery Dataset. The discovery dataset included a total of 323 healthy young Chinese subjects (mean age: 22.7 ± 2.5 y; age range = 18–31 y; 157 males). None of the participants or their first-degree relatives had a history of psychiatric diagnoses, or of neurological or metabolic illnesses, or of drug or alcohol abuse. They all gave full written informed consent to participate in the study. This study was approved by the Ethics Committee of Tianjin Medical University. Eight of the 323 subjects were excluded from further analysis due to genotyping quality control (QC) failure. Our resulting sample comprised 315 individuals with high-quality T1-weighted scans (see table 1 for demographic details).

Replication Dataset. The replication dataset was obtained from a separate cohort of young subjects. A total of 360 healthy Chinese participants (mean age: 19.4 ± 1.1 y; age range = 18–24 y; 186 males) who, together with their first-, second-, and third-degree relatives, had no history of psychiatric disorder were scanned. All of the participants had no history of psychiatric treatment, drug or alcohol abuse,

Table 1. Demographic Characteristics of the Participants

	Discovery Dataset	Replication Dataset
No. of subjects	315	357
Male (%)	48.9	51.3
Age (y)	22.73 ± 2.48	19.41 ± 1.17
Age range (y)	18–31	18–24
Education (y)	15.51 ± 2.66	12.34 ± 0.81

traumatic brain injury, or visible brain lesions on conventional magnetic resonance imaging (MRI). They all gave full written informed consent to participate in the study. This study was approved by the Ethics Committee of the School of Life Science and Technology at the University of Electronic Science and Technology of China. Three of the 360 subjects were excluded from further analysis due to genotyping QC failure, which resulted in a sample comprising 357 participants (see table 1 for demographic details).

Genotype Processing

We collected ethylene diamine tetraacetic acid (EDTA) anti-coagulated venous blood samples from all the participants and then extracted genomic DNA from their whole blood using the EZgene Blood gDNA Miniprep Kit. The whole-genome genotyping was performed on Illumina Human OmniZhongHua-8 BeadChips using the standard Illumina genotyping protocol (Illumina). We performed the subsequent genotype QC using PLINK version 1.07.²⁶ First, we removed the individuals whose missing genotype rates were greater than 0.05 (3 samples from discovery dataset and 1 sample from replicate dataset). Then, we identified the individuals with possible relative relationships by using the estimate of pairwise identity-by-descent (IBD) to find pairs of individuals who had more similar genotypes than we would have expected by chance in a random sample and removed the one of each pair who had the greater missing genotype rate (5 samples from discovery dataset and 2 samples from replicate dataset). Next, we applied single nucleotide polymorphism (SNP)-level filtering, removing SNPs with missing genotype rates greater than 0.05, a minor allele frequency less than 0.01, and significant departure from Hardy–Weinberg Equilibrium ($P < .001$). To control for population stratification, we carried out a principal component analysis (PCA) using EIGENSTART 5.0.2^{27,28} on a linkage disequilibrium (LD) pruned set of autosomal SNPs obtained by carrying out LD pruning with PLINK and removing 5 long-range LD regions with the HapMap phase 3 reference data set.²⁹ After getting 10 principal components, we excluded the outliers of the samples >6 SD. Ugenotyped SNPs were imputed using SHAPEIT v2 (r790)³⁰ and IMPUTE2³¹ with the 1000 Genomes Phase 1 reference dataset. Further analyses focused on autosomal SNPs with imputation quality

scores greater than 0.8. After the QC procedures, 315 and 357 subjects with more than 7 million SNPs remained for the subsequent analyses.

Computation of PGRS

We used the “score” utility in PLINK and the GWAS results²³ to compute the polygenic schizophrenia-risk score. The PGRS was computed following the method developed by Purcell and colleagues,⁴ as described in full detail by Avram and colleagues.³² Since a lower P -value threshold maximizes the predictive ability of a polygenic analysis sample as the discovery GWAS case-control sample increases,⁷ we obtained the list of SNPs that showed a nominal association with schizophrenia ($P < 10^{-3}$) from the GWAS results and evaluated 5 different threshold values: 10^{-3} , 10^{-4} , 10^{-5} , 10^{-6} , and 10^{-7} , yielding 5 different PGRSs.

Choosing the P -threshold to define PGRS is an important step, and some estimation methods have been proposed to define the threshold.^{33,34} However, these methods couldn't work in our high-dimensional MRI data (about 327 684 vertices) of healthy individuals since this is a data-driven study and there are no predefined phenotypes.

In general, a more stringent cutoff generates a score consisting of a smaller number of SNPs with a higher proportion of them being truly related with schizophrenia. On the other hand, by relaxing the threshold, we could increase the number of truly associated SNPs, thus increasing the effect size of PGRS and improving the statistical power for detecting the associations with disease correlates. However, too weak thresholds would include some variants which were too weakly associated with schizophrenia, thus decreasing the statistical power to identify the genetic associations with intermediate phenotypes.³⁵ Therefore, we choose the middle one (10^{-5}) in our analysis, as done in other studies.³⁵

Image Acquisition and Processing

In this study, we finished the image acquisition of each scanner within 6 months, which is a relatively short period of time. During each scanning period, the same sequence and protocol was kept for each subject and no hardware and system upgrade was guaranteed for each scanner. Images from the discovery dataset were acquired with a 3.0 T Signa HDx GE scanner. A 3-dimensional T1-weighted volumetric sequence was performed using a protocol with repetition time (TR) = 8.1 ms, echo time (TE) = 3.1 ms, flip angle (FA) = 13°, field of view (FOV) = 256 × 256 mm², acquisition matrix = 256 × 256, slice thickness = 1 mm without gap, slice number = 176. The replication dataset was acquired with a 3.0 T MR750 GE scanner. A 3-dimensional T1-weighted volumetric sequence was performed using a protocol with TR = 8.16 ms, TE = 3.18 ms, FA = 7°, FOV = 256 × 256 mm², acquisition matrix = 256 × 256, slice thickness = 1 mm without gap, slice number = 188.

The LGI for each vertex quantifies the amount of cortex buried within the sulci on gray matter/cerebrospinal fluid (pial) cortical surface as compared to the amount of cortex that is visible on the outer surface of a 3D circular region of interest (ROI) centered at this vertex.³² The calculation of LGI across the brain was undertaken using the publicly available FreeSurfer software package, version 5.3.0 (<http://surfer.nmr.mgh.harvard.edu/>). Initially, gray matter/white matter (white) and pial surface triangulations were reconstructed.³⁰ The generated cortical surfaces were then carefully reviewed and manually edited for technical accuracy. Vertex-wise estimates of the LGI on the pial surface were calculated using the following steps²¹: (1) creation of an outer smoothed surface tightly wrapping the pial surface; (2) successive estimations of circular 3D ROI with a radius of 25 mm on the outer smoothed surface and of their corresponding circular patches on the pial surface; and (3) computation of the ratio between the areas of the 2 corresponding ROIs at each vertex of the outer smoothed surface and propagations of the LGI values from the outer smoothed surface to the pial cortical surface. In this way, values ranging from 1 to 5 were assigned to each vertex representing the degree of cortical folding on a regional scale. Higher LGI indicates extensive folding whereas a LGI value of 1 means a flat cortex. For comparison, all of the individual LGI maps were aligned to an average template by using a surface-based registration algorithm.³⁶ We used a full-width at half-maximum of 20 mm to smooth the vertex-wise maps.

Statistical Analysis

Vertex-wise analyses of LGI were performed using a general linear model controlling for the effect of age and gender to estimate the association between the LGI measure at each vertex and the PGRS for the discovery and replication datasets separately. A total of 163 842 vertices for each hemisphere were tested for associations with PGRS. To correct for multiple comparisons, a Monte Carlo cluster simulation and a cluster analysis were performed to identify the clusters with significant cortical complexity.³¹ The algorithm of cluster-wise correction for multiple comparisons by a Monte Carlo simulation was implemented in the framework of FreeSurfer software package. The method used a simulation to obtain a measure of the distribution of the maximum cluster size under the null hypothesis.³⁷ To be specific, the simulation populated the cortical surface with normally distributed random data, thresholded the data with vertex-wise threshold, and applied the smoothness of the actual data. The area of the largest cluster was then calculated. By repeating this process for a given number of iterations, a histogram of maximum cluster area that occurred for random data of a given smoothness was generated. A corrected P value for the cluster size was computed, indicating the probability of seeing a maximum cluster of that size or larger. Clusters remaining in the areas of significance to the LGI

maps show that the result is not likely due to chance. In our analysis, a total of 10 000 iterations were performed in the simulation procedure, using a vertex-wise threshold of $P < .05$ and a cluster-wise threshold of $P < .05$.

The anatomical overlap of brain regions with significant correlations between the LGI and the PGRS using the discovery and replication datasets was determined by a conjunction analysis.³⁸ This facilitated inspection to see if the regions with significant correlations produced by the 2 independent datasets were consistent.

A Pearson correlation was further performed to test the association between the mean LGI of the identified clusters and the PGRS with age and gender as covariates.

Results

Associations Between the LGI and the PGRS in the Discovery Dataset

The demographic information is shown in table 1. We first investigated the effects of the PGRS on the LGI based on the data from 315 young healthy subjects and found significant negative correlations between the PGRS and the LGI in 2 clusters, one in each hemisphere (figure 1A, corrected cluster-wise $P = .026$ for the cluster in the left hemisphere, corrected cluster-wise $P < .001$ for the cluster

in the right hemisphere). These clusters involved the bilateral IPL, the right postcentral areas, and a portion of the precentral areas. There were no significant positive associations between the LGI and the PGRS.

Associations Between the LGI and the PGRS in the Replication Dataset

In addition, we performed the same kinds of analyses on the data from the 357 independent replication subjects. We observed 2 similar clusters, one in each hemisphere, that had significant negative correlations between the LGI and the PGRS (figure 1B, corrected cluster-wise $P = .006$ for the cluster in the left hemisphere, corrected cluster-wise $P < .001$ for the cluster in the right hemisphere). These clusters involved the bilateral IPLs, the left lateral occipital, parts of the right postcentral and precentral areas extending to the middle frontal, and the inferior frontal regions. There were no significant positive associations between the LGI and the PGRS. Supplementary table 1 shows clusters with significant associations between LGI and PGRS in discovery and replication datasets.

Conjunction Analysis of Regions With Joint Significant Associations Using the Discovery and Replication Datasets

A conjunction analysis indicated that the 2 independent datasets produced consistent regions with significant negative correlations. These regions were primarily located in the IPL, including the bilateral supramarginal and angular gyri (figure 1C). The association between the mean LGI within the IPL and the PGRS in the discovery and replication datasets is shown in figure 2. The PGRS accounts for 1.5% variation of the LGI within left IPL and 2% variation of the LGI within right IPL in the discovery datasets, while in the replication dataset, the PGRS accounts for 1% variation of LGI within left IPL and 2.1% variation of the LGI within right IPL. Supplementary table 2 shows the associations between PGRSs and mean LGI within the significant clusters by taking age and gender as covariates and these results support our choice about threshold.

Discussion

The present study revealed a consistent effect of the polygenic risk for schizophrenia on cortical gyrification in the IPL in 2 independent general-population samples. A higher PGRS was significantly associated with a lower LGI in the bilateral IPL, areas that have previously been linked to schizophrenia in case-control studies.³⁹ These findings support our hypothesis. The fact that these results were robust in that they were very similar in the 2 independent populations suggests that reduced IPL gyrification, which may imply abnormal neurodevelopment in the IPL, is a genetically modulated vulnerability factor that is likely associated with schizophrenia.

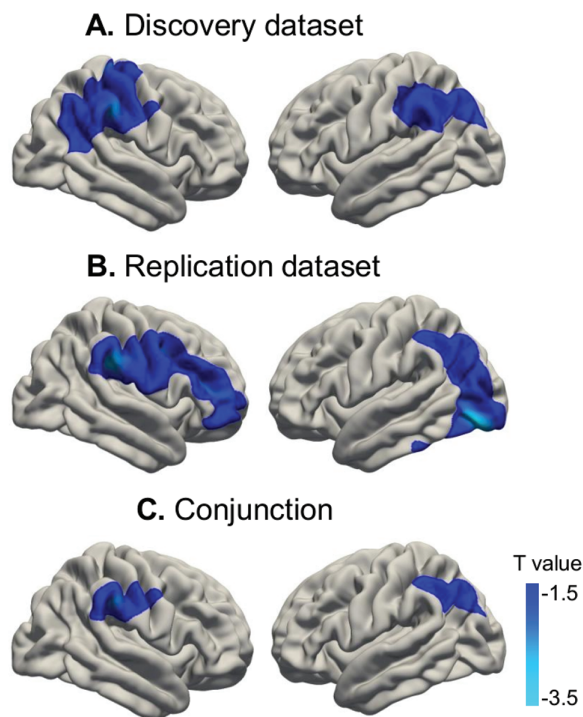


Fig. 1. Associations between local gyrification index (LGI) and polygenic risk score (PGRS) using discovery dataset (A), replication dataset (B), and the conjunction analysis for the regions with joint significant associations using discovery and replication datasets (C). The regions in blue showed a significant linear decrease in LGI with increasing PGRS. The color bar indicates T -values corrected for cluster-wise multiple comparisons with $P < .05$.

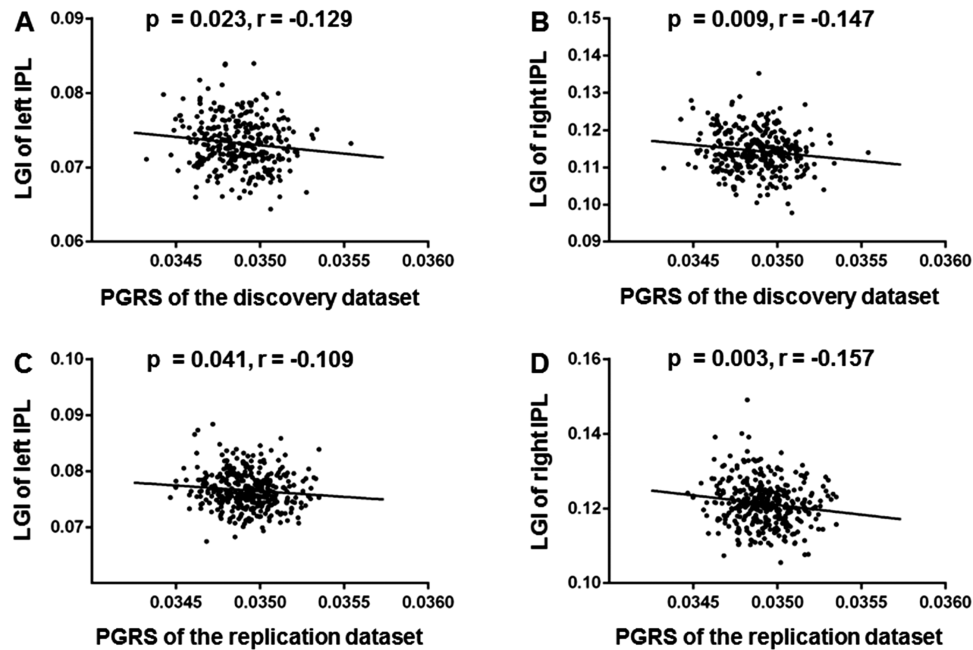


Fig. 2. Individual local gyrification index (LGI) within the bilateral inferior parietal lobule (IPL) from conjunction analysis was significantly negatively associated with polygenic risk score (PGRS) for schizophrenia in both discovery dataset and replication dataset: (A) left IPL of discovery dataset; (B) right IPL of discovery dataset; (C) left IPL of replication dataset; (D) right IPL of replication dataset. *P* values are shown with age and gender as covariates.

Apart from the aforementioned studies which investigated whether abnormal brain function and cognitive impairment could be attributed to the polygenic architecture of schizophrenia, 3 additional studies examined the combined effect of schizophrenia-related loci on brain volume. Unfortunately, they reported contradictory results: One of them found a negative association between brain volume and the polygenic risk for schizophrenia,¹³ whereas the 2 other studies did not find any association.^{14,15} However, assessing only cortical volume may obscure individual differences in other cortical morphological measures⁴⁰ such as cortical gyrification. Cortical gyrification refers to the neurodevelopmental process by which the cortical morphology is altered to form sulcal and gyral regions⁴¹ and may reflect optimal intra-cortical organizations.⁴² Previous longitudinal studies of cortical gyrification have found that by the age of 2, the cortical gyrification increases 23.7% compared with the value at birth, may peak between 2 and 6 years old,⁴³ and then decreases in most of the brain surface.^{44,45} So we speculate that lower LGI in higher risk adults may result from abnormal increase before 6 years old or excessive decrease after that period. However, more biological evidences are needed to reveal the specific mechanisms of the current finding. Since schizophrenia is now widely accepted as having neurodevelopmental origins, investigating the direct influences of genetic factors involved in neurodevelopmental process on cortical gyrification could help further understand the etiopathology of schizophrenia. By combining the effects of tens of thousands of weakly-associated risk variants for schizophrenia

into a single risk score, we were able to detect the cumulative effects of various biological systems and pathways which might influence cortical gyrification. Taken together, our results seem to further support a model in which genetic variants increase the risk for schizophrenia through abnormal development of cortical structure.

In this study we found that subjects with a higher polygenic risk for schizophrenia showed a lower LGI in the IPL. Previous studies have investigated the differences of cortical gyrification between schizophrenia patients and normal controls, and majority of studies reported hypoglyria of LGI in patients.⁴⁶ Reduced gyrification in the IPL has been reported in schizophrenics compared to healthy controls.^{39,47} In another study, significant hypoglyria was found in the right inferior parietal lobe in schizoaffective individuals compared to normal subjects and a trend toward hypoglyria was found in the right IPL of schizophrenics compared to control subjects.⁴⁶ In addition, a decreased LGI in the IPL was found in individuals with velo-cardio-facial syndrome, who are at high risk for developing schizophrenia, compared to normal controls.⁴⁸ The IPL is involved in several functions, including executive functions,^{49–51} working memory,^{52,53} and social cognition.⁵⁴ Varieties of clinical symptoms, such as thought disorder, disturbance of body image, disruptions in the sense of self, and attention deficits, suggest a role for the abnormalities of the IPL⁵⁵ in schizophrenia. Furthermore, the IPL forms an integral part of the critical fronto-parietal network, which has been implicated in various cognitive deficits and clinical symptoms in schizophrenia.⁵⁶

Thus, the IPL has emerged as a prominent neuroanatomical location for the therapeutic application of repetitive transcranial magnetic stimulation in schizophrenia.^{57,58} Our results may suggest that common genetic variants of schizophrenia affect the cortical morphometry of the IPL and thus increase schizophrenia vulnerability.

Besides the IPL, we also found significant association in the precentral and postcentral regions. Motor dysfunction is one of the major features of schizophrenia.^{59–61} Movement is accompanied by activation of the postcentral gyrus and somatosensory stimuli that activate the precentral gyrus.⁶² Given that the primary motor cortex (precentral and postcentral gyrus) is responsible for the direct production of motor and its outputs to the pyramidal tract, any gray matter or white matter loss in this area could produce a movement deficit.⁵⁹ Moreover, precentral areas are involved in the pathophysiology of abnormal social communication in schizophrenia patients.⁶³ Our structural MRI studies showed lower LGI in these areas in higher risk adults, which corroborates previous studies showing abnormal activation, volume loss and abnormalities in cortical gyrification in these brain regions in the schizophrenia patients.^{24,59,63,64} Except for the regions showing differences in our studies, previous studies also found other brain areas, including frontal cortex,^{65,66} showing differences in cortical gyrification. Moreover, we found the replication dataset showed a greater extent of cortical areas associated with PGRS. Sample differences in age, education level and other environmental factors may make such differences in results. However, more solid evidences are needed to support such explanations.

Our study found a consistent relationship between the PGRS and cortical gyrification. However, several issues still need to be considered and future studies should address these. First, increasing the sample size in a future study can improve the statistical results of a polygenic analysis.⁶ Second, since the PGRS was derived by analyzing each candidate locus independently and then aggregating the data into an additive model,⁴ we did not consider potential gene-gene interactions. Future studies should investigate epistatic effects by using more sophisticated multivariate models. Third, the list of SNPs used for computing the PGRS was derived from a single GWAS because, in this way, we were able to obtain a complete list of the SNPs and their corresponding odds ratios from what is currently the largest GWAS of schizophrenia. Future research should include additional SNPs that have been identified by other studies. Fourth, although the discovery sample and the replicate sample are both scanned on 3.0T GE Scanners and the sequences used in 2 scanners are almost similar, more stringent QC protocol should be performed in further studies. For example, a few subjects could have been scanned on both scanners for examination and correction, and the longitudinal QC within each scanner also should be considered. Fifth,

both discovery sample and replication sample were young adults, however, age was significantly different between the 2 datasets. Though we have taken age as one of covariates in the statistical analysis, more evidences and independent samples are needed to find the effect of age on the results in the future studies. Finally, if we could calculate the PGRS based on a Chinese GWAS in the future, it may improve the statistical power.

In conclusion, we found a robust relationship between a greater polygenic risk for schizophrenia and a lower level of cortical gyrification in the IPL in 2 independent samples. Our results support a number of studies which have demonstrated a polygenic etiology for schizophrenia and related phenotypes. We were also able to strongly support the effectiveness of 2 approaches, PGRS and endophenotype analysis, in establishing the genetic architecture of psychiatry.

Supplementary Material

Supplementary material is available at <http://schizophreniabulletin.oxfordjournals.org>.

Funding

This work was supported by the National Key Basic Research and Development Program (973) (Grant No. 2011CB707800), the Strategic Priority Research Program of the Chinese Academy of Sciences (Grant No. XDB02030300), the Natural Science Foundation of China (Grant Nos. 91232718 and 91132301).

Acknowledgments

We thank Drs Rhoda E and Edmund F. Perozzi for English and content editing assistance and discussions. All of the authors declare no competing interests.

References

- Escudero I, Johnstone M. Genetics of schizophrenia. *Curr Psychiatry Rep.* 2014;16:502.
- Ripke S, O'Dushlaine C, Chambert K, et al. Genome-wide association analysis identifies 13 new risk loci for schizophrenia. *Nature Genet.* 2013;45:1150–1159.
- Munafo MR, Bowes L, Clark TG, Flint J. Lack of association of the COMT (Val158/108 Met) gene and schizophrenia: a meta-analysis of case-control studies. *Mol Psychiatry.* 2005;10:765–770.
- Purcell SM, Wray NR, Stone JL, et al; International Schizophrenia C. Common polygenic variation contributes to risk of schizophrenia and bipolar disorder. *Nature.* 2009;460:748–752.
- Dima D, Breen G. Polygenic risk scores in imaging genetics: usefulness and applications. *J Psychopharmacology.* 2015;29:867–871.
- Dudbridge F. Power and predictive accuracy of polygenic risk scores. *PLoS Genet.* 2013;9:e1003348.

7. Wray NR, Lee SH, Mehta D, Vinkhuyzen AA, Dudbridge F, Middeldorp CM. Research review: polygenic methods and their application to psychiatric traits. *J Child Psychol Psychiatry*. 2014;55:1068–1087.
8. Derks EM, Vorstman JA, Ripke S, Kahn RS, Ophoff RA; Schizophrenia Psychiatric Genomic Consortium. Investigation of the genetic association between quantitative measures of psychosis and schizophrenia: a polygenic risk score analysis. *PLoS One*. 2012;7:e37852.
9. Hatzimanolis A, Bhatnagar P, Moes A, et al. Common genetic variation and schizophrenia polygenic risk influence neurocognitive performance in young adulthood. *Am J Med Genet B Neuropsychiatr Genet*. 2015;168:392–401.
10. McIntosh AM, Gow A, Luciano M, et al. Polygenic risk for schizophrenia is associated with cognitive change between childhood and old age. *Biol Psychiatry*. 2013;73:938–943.
11. Walton E, Geisler D, Lee PH, et al. Prefrontal inefficiency is associated with polygenic risk for schizophrenia. *Schizophr Bull*. 2014;40:1263–1271.
12. Kauppi K, Westlye LT, Tesli M, et al. Polygenic risk for schizophrenia associated with working memory-related prefrontal brain activation in patients with schizophrenia and healthy controls. *Schizophr Bull*. 2015;41:736–743.
13. Terwisscha van Scheltinga AF, Bakker SC, van Haren NE, et al. Genetic schizophrenia risk variants jointly modulate total brain and white matter volume. *Biol Psychiatry*. 2013;73:525–531.
14. Van der Auwera S, Wittfeld K, Homuth G, Teumer A, Hegenscheid K, Grabe HJ. No association between polygenic risk for schizophrenia and brain volume in the general population. *Biol Psychiatry*. 2015;78:e41–e42.
15. Papiol S, Mitjans M, Assogna F, et al. Polygenic determinants of white matter volume derived from GWAS lack reproducibility in a replicate sample. *Transl Psychiatry*. 2014;4:e362.
16. Rimol LM, Hartberg CB, Nesvag R, et al. Cortical thickness and subcortical volumes in schizophrenia and bipolar disorder. *Biol Psychiatry*. 2010;68:41–50.
17. Palaniyappan L, Liddle PF. Diagnostic discontinuity in psychosis: a combined study of cortical gyrification and functional connectivity. *Schizophr Bull*. 2014;40:675–684.
18. Mier D, Kirsch P, Meyer-Lindenberg A. Neural substrates of pleiotropic action of genetic variation in COMT: a meta-analysis. *Mol Psychiatry*. 2010;15:918–927.
19. Preston GA, Weinberger DR. Intermediate phenotypes in schizophrenia: a selective review. *Dialogues Clin Neurosci*. 2005;7:165–179.
20. White T, Gottesman I. Brain connectivity and gyrification as endophenotypes for schizophrenia: weight of the evidence. *Curr Top Med Chem*. 2012;12:2393–2403.
21. Schaer M, Cuadra MB, Tamarit L, Lazeyras F, Eliez S, Thiran JP. A surface-based approach to quantify local cortical gyrification. *IEEE Trans Med Imaging*. 2008;27:161–170.
22. Schaer M, Cuadra MB, Schmanky N, Fischl B, Thiran JP, Eliez S. How to measure cortical folding from MR images: a step-by-step tutorial to compute local gyrification index. *J Vis Exp*. 2012;59:e3417.
23. Ripke S, O'Donovan MC; Schizophrenia Working Group of the Psychiatric Genomics Consortium. Biological insights from 108 schizophrenia-associated genetic loci. *Nature*. 2014;511:421–427.
24. Nesvag R, Schaer M, Haukvik UK, et al. Reduced brain cortical folding in schizophrenia revealed in two independent samples. *Schizophr Res*. 2014;152:333–338.
25. Palaniyappan L, Mallikarjun P, Joseph V, White TP, Liddle PF. Folding of the prefrontal cortex in schizophrenia: regional differences in gyrification. *Biol Psychiatry*. 2011;69:974–979.
26. Purcell S, Neale B, Todd-Brown K, et al. PLINK: a tool set for whole-genome association and population-based linkage analyses. *Am J Hum Genet*. 2007;81:559–575.
27. Patterson N, Price AL, Reich D. Population structure and eigenanalysis. *PLoS Genet*. 2006;2:e190.
28. Price AL, Patterson NJ, Plenge RM, Weinblatt ME, Shadick NA, Reich D. Principal components analysis corrects for stratification in genome-wide association studies. *Nature Genet*. 2006;38:904–909.
29. Thorisson GA, Smith AV, Krishnan L, Stein LD. The International HapMap Project Web site. *Genome Res*. 2005;15:1592–1593.
30. Delaneau O, Marchini J, Zagury JF. A linear complexity phasing method for thousands of genomes. *Nat Methods*. 2012;9:179–181.
31. Howie BN, Donnelly P, Marchini J. A flexible and accurate genotype imputation method for the next generation of genome-wide association studies. *PLoS Genet*. 2009;5:e1000529.
32. Holmes AJ, Lee PH, Hollinshead MO, et al. Individual differences in amygdala-medial prefrontal anatomy link negative affect, impaired social functioning, and polygenic depression risk. *J Neurosci*. 2012;32:18087–18100.
33. Whalley HC, Sprooten E, Hackett S, et al. Polygenic risk and white matter integrity in individuals at high risk of mood disorder. *Biol Psychiatry*. 2013;74:280–286.
34. Power RA, Steinberg S, Bjornsdottir G, et al. Polygenic risk scores for schizophrenia and bipolar disorder predict creativity. *Nat Neurosci*. 2015;18:953–955.
35. Sabuncu MR, Buckner RL, Smoller JW, Lee PH, Fischl B, Sperling RA; Alzheimer's Disease Neuroimaging I. The association between a polygenic Alzheimer score and cortical thickness in clinically normal subjects. *Cerebral Cortex*. 2012;22:2653–2661.
36. Fischl B, Sereno MI, Tootell RB, Dale AM. High-resolution intersubject averaging and a coordinate system for the cortical surface. *Hum Brain Mapp*. 1999;8:272–284.
37. Hagler DJ Jr, Saygin AP, Sereno MI. Smoothing and cluster thresholding for cortical surface-based group analysis of fMRI data. *Neuroimage*. 2006;33:1093–1103.
38. Nichols T, Brett M, Andersson J, Wager T, Poline JB. Valid conjunction inference with the minimum statistic. *NeuroImage*. 2005;25:653–660.
39. Palaniyappan L, Liddle PF. Dissociable morphometric differences of the inferior parietal lobule in schizophrenia. *Eur Arch Psychiatry Clin Neurosci*. 2012;262:579–587.
40. Wang C, Zhang Y, Liu B, Long H, Yu C, Jiang T. Dosage effects of BDNF Val66Met polymorphism on cortical surface area and functional connectivity. *J Neuroscience*. 2014;34:2645–2651.
41. White T, Su S, Schmidt M, Kao CY, Sapiro G. The development of gyrification in childhood and adolescence. *Brain Cogn*. 2010;72:36–45.
42. Caviness VS Jr. Mechanical model of brain convolutional development. *Science*. 1975;189:18–21.
43. Li G, Wang L, Shi F, et al. Mapping longitudinal development of local cortical gyrification in infants from birth to 2 years of age. *J Neurosci*. 2014;34:4228–4238.
44. Hogstrom LJ, Westlye LT, Walhovd KB, Fjell AM. The structure of the cerebral cortex across adult life: age-related

- patterns of surface area, thickness, and gyrification. *Cereb Cortex*. 2013;23:2521–2530.
45. Raznahan A, Shaw P, Lalonde F, et al. How does your cortex grow? *J Neurosci*. 2011;31:7174–7177.
 46. Nanda P, Tandon N, Mathew IT, et al. Local gyrification index in probands with psychotic disorders and their first-degree relatives. *Biol Psychiatry*. 2014;76:447–455.
 47. Palaniyappan L, Liddle PF. Aberrant cortical gyrification in schizophrenia: a surface-based morphometry study. *J Psychiatry Neurosci*. 2012;37:399–406.
 48. Srivastava S, Buonocore MH, Simon TJ. Atypical developmental trajectory of functionally significant cortical areas in children with chromosome 22q11.2 deletion syndrome. *Hum Brain Map*. 2012;33:213–223.
 49. Buchsbaum BR, Greer S, Chang WL, Berman KF. Meta-analysis of neuroimaging studies of the Wisconsin card-sorting task and component processes. *Hum Brain Map*. 2005;25:35–45.
 50. Collette F, Olivier L, Van der Linden M, et al. Involvement of both prefrontal and inferior parietal cortex in dual-task performance. *Brain Res Cogn Brain Res*. 2005;24:237–251.
 51. Salgado-Pineda P, Baeza I, Perez-Gomez M, et al. Sustained attention impairment correlates to gray matter decreases in first episode neuroleptic-naïve schizophrenic patients. *NeuroImage*. 2003;19:365–375.
 52. Kindermann SS, Brown GG, Zorrilla LE, Olsen RK, Jeste DV. Spatial working memory among middle-aged and older patients with schizophrenia and volunteers using fMRI. *Schizophr Res*. 2004;68:203–216.
 53. Jansma JM, Ramsey NF, van der Wee NJ, Kahn RS. Working memory capacity in schizophrenia: a parametric fMRI study. *Schizophr Res*. 2004;68:159–171.
 54. Decety J, Sommerville JA. Shared representations between self and other: a social cognitive neuroscience view. *Trends Cogn Sci*. 2003;7:527–533.
 55. Torrey EF. Schizophrenia and the inferior parietal lobule. *Schizophr Res*. 2007;97:215–225.
 56. Li Y, Liu B, Hou B, et al. Less efficient information transfer in Cys-allele carriers of DISC1: a brain network study based on diffusion MRI. *Cereb Cortex*. 2013;23:1715–1723.
 57. Uddin LQ, Molnar-Szakacs I, Zaidel E, Iacoboni M. rTMS to the right inferior parietal lobule disrupts self-other discrimination. *Soc Cogn Affect Neurosci*. 2006;1:65–71.
 58. Freitas C, Fregni F, Pascual-Leone A. Meta-analysis of the effects of repetitive transcranial magnetic stimulation (rTMS) on negative and positive symptoms in schizophrenia. *Schizophr Res*. 2009;108:11–24.
 59. Singh S, Goyal S, Modi S, et al. Motor function deficits in schizophrenia: an fMRI and VBM study. *Neuroradiology*. 2014;56:413–422.
 60. Pappa S, Dazzan P. Spontaneous movement disorders in antipsychotic-naïve patients with first-episode psychoses: a systematic review. *Psychol Med*. 2009;39:1065–1076.
 61. Fenton WS. Prevalence of spontaneous dyskinesia in schizophrenia. *J Clin Psychiatry*. 2000;61(suppl 4):10–14.
 62. Cramer SC, Moore CI, Finklestein SP, Rosen BR. A pilot study of somatotopic mapping after cortical infarct. *Stroke*. 2000;31:668–671.
 63. Watanuki T, Matsuo K, Egashira K, et al. Precentral and inferior prefrontal hypoactivation during facial emotion recognition in patients with schizophrenia: a functional near-infrared spectroscopy study. *Schizophr Res*. 2016;170:109–114.
 64. Palaniyappan L, Park B, Balain V, Dangi R, Liddle P. Abnormalities in structural covariance of cortical gyrification in schizophrenia. *Brain Struct Funct*. 2015;220:2059–2071.
 65. Narr KL, Bilder RM, Kim S, et al. Abnormal gyral complexity in first-episode schizophrenia. *Biol Psychiatry*. 2004;55:859–867.
 66. Prasad KM, Goradia D, Eack S, et al. Cortical surface characteristics among offspring of schizophrenia subjects. *Schizophr Res*. 2010;116:143–151.